Plant Stress 21 (2026) 101382

Contents lists available at ScienceDirect

Plant Stress

journal homepage: www.sciencedirect.com/journal/plant-stress

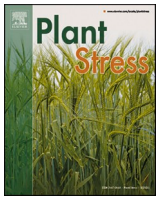

Volatile-mediated allelopathy: *Perovskia atriplicifolia* Benth. volatile organic compounds trigger phenylpropanoid–lignin remodelling in *Amaranthus retroflexus* L.

Alice Zambelli [a,1], Emanuela Talarico [b,1], Cristina Teruzzi [a], Eleonora Greco [b], David López-González [c,d], Yedra Vieites-Álvarez [c,d], Ahmad Arzani [e], Sara Álvarez-Rodríguez [c,d], Fabio F. Nocito [a], Leonardo Bruno [b], Fabrizio Araniti [a,*]

[a] Dipartimento di Scienze Agrarie e Ambientali - Produzione, Territorio, Agroenergia, Università degli Studi di Milano, 20133 Milano, Italy
[b] Department of Biology, Ecology and Earth Sciences (DiBEST), University of Calabria, 87036 Rende, Italy
[c] Departamento de Bioloxía Vexetal e Ciencia do Solo, Facultade de Bioloxía, Universidade de Vigo, Campus Lagoas-Marcosende s/n, Vigo 36310, Spain
[d] Instituto de Agroecoloxía e Alimentación (IAA), Campus Auga, Ourense 32004, Spain
[e] Department of Agronomy and Plant Breeding, College of Agriculture, Isfahan University of Technology, Isfahan 8415683111, Iran

ARTICLE INFO

Keywords:
Allelopathy
Secondary metabolism
Phenylpropanoids
Cuticular waxes
Metabolomics
Plant–plant interactions

ABSTRACT

This study investigated the allelopathic effects of volatile organic compounds (VOCs) emitted by *Perovskia atriplicifolia* Benth. on the weed *Amaranthus retroflexus L.*. Headspace SPME-GC-MS identified 70 VOCs, mainly o-cymene (~33%), δ-3-carene (~15%), and 1,8-cineole (~8%), in *P. atriplicifolia*. Bioassays revealed strong inhibitory effects: germination was reduced by approximately 40% at 100 g and 62% at 200 g of *P. atriplicifolia* biomass, while root length decreased by more than 60% at both doses. At doses around the ED_{50}, treated seedlings developed reduced fresh weight (−16%), lower relative water content (−13%), and higher osmotic potential (+16%). Cuticular analyses indicated a shift toward long-chain aliphatics, and metabolomics showed increased accumulation of phenylpropanoid intermediates (e.g., sinapic, ferulic, *p*-coumaric acids) together with higher PAL activity (+52%), PPO activity (+180%), total phenolic and lignin content (+61%).

Overall, *P. atriplicifolia* VOCs, dominated by o-cymene, δ-3-carene, and 1,8-cineole, significantly impair the germination and early growth of *A. retroflexus*, triggering metabolic reprogramming toward phenylpropanoid–lignin biosynthesis and cuticular reinforcement. This study advances the understanding of volatile-mediated allelopathy by linking biochemical profiles to integrative physiological and metabolomic responses in *A. retroflexus* plants.

1. Introduction

Plants are widely recognised for emitting volatile organic compounds (VOCs) from all their organs (Bergman et al., 2025). While constitutive VOC emissions are generally modest, they can increase markedly in response to biotic stresses, such as herbivore feeding or pathogen attack, as well as to abiotic factors, including drought and heat (Yang et al., 2025; Wielkopolan et al., 2025). Once released, VOCs act as multifunctional signaling molecules that mediate interactions within and between species (Mobarak et al., 2025; Araniti et al., 2017). Beyond plant–plant and plant–herbivore interactions, VOCs also play a relevant role in microbially mediated processes, such as solid-state fermentations, where microbial succession and strain-specific activity shape volatile fingerprints and product quality (Gao et al., 2025; Xiao et al., 2024; Xiao et al., 2022). These interactions can occur through active mechanisms, where recipient plants undergo molecular or physiological changes, or through passive mechanisms, in which volatiles adhere to plant surfaces without necessarily eliciting direct responses (Brosset and Blande, 2022; Li et al., 2012).

Plant volatiles play diverse ecological roles and serve as key

* Corresponding author at: Dipartimento di Scienze Agrarie e Ambientali - Produzione, Territorio, Agroenergia (Di.S.A.A.), Università degli Studi di Milano, Via Celoria, 2, 20133 Milano, Italy.
E-mail address: fabrizio.araniti@unimi.it (F. Araniti).
[1] Both authors equally contributed to the manuscript.

https://doi.org/10.1016/j.stress.2026.101382
Received 24 November 2025; Received in revised form 2 March 2026; Accepted 13 April 2026
Available online 14 April 2026

mediators of mutualistic interactions between plants and their biological and physical surroundings. Terpenoids are among the most abundant and functionally diverse plant volatile compounds (Arzani et al., 2025). They contribute to plant defence by deterring herbivores and pathogens, facilitate pollination, and serve as cues in interplant communication (Pierik et al., 2014; Ninkovic et al., 2021; Effah et al., 2019). Beyond these roles, a growing body of evidence has demonstrated their involvement in allelopathy, the ability of plants to interfere with neighbouring species through chemical interactions. Volatile allelochemicals can delay or inhibit seed germination and seedling growth, effects that strongly influence competitive balance and community assembly (Araniti et al., 2017; Verdeguer et al., 2020; Effah et al., 2019; Landi et al., 2020). Even transient inhibition during early developmental stages may significantly alter the ability of one species to establish itself in the presence of others (Karban, 2007; Wang et al., 2022).

Muller and Muller (1964) first demonstrated that the growth inhibition of grassland species near *Salvia leucophylla* colonies was mainly due to monoterpenes such as camphor and cineole. Subsequent studies confirmed that terpenoids emitted by *S. leucophylla* and other aromatic shrubs could suppress plant growth by acting on cell division, DNA synthesis, and microbial dynamics in soils (Nishida et al., 2005; Karban, 2007). More recent work has extended these findings to Mediterranean shrubs, such as *Dittrichia viscosa*, whose volatile emissions have been shown to impair neighbour metabolism, induce oxidative bursts, and damage photosynthetic machinery (Araniti et al., 2017). Together, these studies underscore how VOCs can act as modulators of plant homeostasis and drivers of vegetation dynamics.

Within this context, the Lamiaceae family has been one of the most extensively studied groups for the production, release, and ecological function of VOCs (Haas et al., 2024; Gladikostić et al., 2023; Rattray and Van Wyk, 2021).

Recent manuscripts have highlighted the remarkable chemical diversity of Lamiaceae volatiles, particularly the dominance of mono- and sesquiterpenes and their ecological roles in plant defence, stress tolerance, interspecific interactions, and allelopathy (Haas et al., 2024; de Souza et al., 2022; Islam et al., 2022; Linhart et al., 2015; Gershenzon & Dudareva, 2007). These studies emphasise the importance of volatile-mediated mechanisms within this family and underscore the need to investigate species-specific volatile blends and their biological effects.

P. atriplicifolia Benth., commonly known as Russian sage, is a perennial aromatic subshrub belonging to this family. Native to Central Asia, particularly Afghanistan, Pakistan, and Tibet, it has spread widely as an ornamental plant due to its high resilience to drought and nutrient-poor soils (Samani et al., 2025; Gostin and Popescu, 2025). Its foliage, rich in glandular trichomes, produces a complex mixture of terpenoid compounds, such as camphor and 1,8-cineole, which have been associated with defence, stress tolerance, and allelopathic interactions (Verdeguer et al., 2020). Despite the well-documented bioactive potential of its extracts, the ecological role of *P. atriplicifolia* foliage volatiles in plant–plant interactions remains largely unexplored.

Here, we assess the allelopathic potential of *P. atriplicifolia* VOCs against *A. retroflexus*, a fast-growing, invasive C4 weed. *A. retroflexus* is notorious for its prolific seed production, rapid establishment, and wide ecological tolerance, making it a significant competitor in agricultural systems (Costea et al., 2004; Guo and Al-Khatib, 2003). By combining controlled microcosm experiments with metabolomic profiling, this study investigates the effects of naturally released *P. atriplicifolia* volatiles on the germination, root development, and seedling physiology of *A. retroflexus*. This integrative approach aims to provide novel insights into the phytochemical ecology of *P. atriplicifolia* and its potential role in shaping plant community dynamics through volatile-mediated allelopathy.

2. Materials and methods

2.1. Seed and seedling growth experiments

2.1.1. Headspace-solid phase micro extraction-GC-MS analysis of plant volatiles

The VOCs released by *P. atriplicifolia* were chemically characterised through the HS-SPME-GC-MS method using a Thermo Fisher gas chromatograph apparatus (Trace 1310) coupled to a single quadrupole mass spectrometer (ISQ LT) and a Tri-Plus RSH autosampler. A MEGA-5MS (30 m×0.25 mm×0.25μm + 10 m of pre-column) column was used for sample chromatography, and ultra-pure helium (6.0) with a flow rate of 1 ml/min was used as the gas carrier. The source and injector were set to 260°C and 200°C, respectively.

Plants were grown in Reggio Calabria (Italy), in an open field at the University Mediterranea of Reggio Calabria, and were collected in May, just before the flowering period (balsamic period) in which the yield of essential oils is at its maximum (Dabiri and Sefidkon, 2001). For the experiments, only fully developed leaves were used.

One gram of plant material was sealed in a 20 ml glass vial and equilibrated at room temperature for 20 minutes. A grey SPME fiber (StableFlex, divinylbenzene/Carboxen on polydimethylsiloxane coating; 50/30 μm coating; Supleco) was used for sample absorption. The fiber was exposed to plant VOCs for 30 minutes to allow chemical adsorption. Successively, the extracted sample was injected into the GC-MS apparatus in a split mode with a split ratio of 1: 60. Sample separation was achieved using the following temperature ramp: 7 minutes at 45°C, from 45°C to 80°C with a rate of 10°C×min, from 80°C to 200°C with a rate of 20°C×min then isocratic for 3 minutes 200°C.

Mass spectra were recorded in electronic impact (EI) mode at 70 eV. The analysis was carried out in full scan mode, from 45 to 500 m/z. The retention index (RI) was calculated using an *n*-alkane standard mixture (C10-C30 all-even) separately injected.

The sample was injected three times, and the obtained chromatograms were aligned and deconvoluted using the open-source software MS-DIAL 4.8. The area of each compound was extracted and mediated. The peak annotation was achieved using the RI and spectral similarity matching with a cosine score cut-off of 70% using an in-house EI spectral library (Misra, 2019), following the Metabolomics Standards Initiative of the International Metabolomics Society. In particular, as suggested by Sumner et al. (2007), the annotations were considered at level 2 (putative annotation based on spectral library similarity) or level 3 (putatively characterised compound class based on spectral similarity to known compounds of a chemical class).

2.1.2. In vitro VOCs bioassays

The *in vitro* volatiles bioassay was carried out as previously described by Araniti et al. (2017), with some modifications. Freshly harvested leaves were evaluated for their volatiles' phytotoxic activity, permitting only atmospheric contact between the donor (*Perovskia atriplicifolia* Benth.) and the receiver species (*Amaranthus retroflexus* L.). The aerial parts (0, 25, 50, 100, and 200 g) of *P. atriplicifolia* were collected and immediately placed on the bottom of a 4 L glass container capped with a net, for a detailed description of the system look at Araniti et al. (2017). The *P. atriplicifolia* plant material was covered by a stay-up metal net on which Petri dishes (6 cm in Diameter), filled with filter paper and moistened with 2 mL of sterile deionised water, were gently placed. The container was then transferred to a climatic chamber, set with 16 hours of light at 30°C and 8 hours of dark at 20°C, with a photon flux density of 230 μmol m^{-2} s^{-1}. For each petri dish, 20 sterilised seeds of *Amaranthus retroflexus* L. were sown. Germinated seeds were counted daily for 5 days, considering those seeds with a root protrusion of≥ 1 mm as germinated. Total Germination (%) and speed of germination were calculated using the formulas reported in the following review (Chiapusio et al., 1997).

Total root growth (cm) was evaluated after 48 hr of treatment on five

pre-germinated seedlings, chosen for uniformity and grown as previously described for the experiment on seed germination. *P. atriplicifolia* plant material was changed daily using freshly cut branches.

The dose-response curves for both physiological processes studied (germination and root growth) were used to calculate the ED_{50} (dose inhibiting 50% of the parameter under study; see the statistical analysis chapter). This value (expressed in grams of fresh-cut material) was used in the subsequent experiment conducted on the developed seedlings.

2.2. Bioassays on established seedlings

The experiments on well-established seedlings were carried out on *A. retroflexus* germinated in a professional potting soil (Orticole alveolo TecnoGrow, Tercomposti, Calvisano BS, Italy) and grown in individual pots (10 cm in Ø, with a volume of 0.461 L) until the fourth true leaf was formed. Every replicate consisted of 10 plants pooled together at the end of the experiment. The seedlings selected for the treatment were exposed for 10 days to 120 g of plant material (average of the ED_{50} calculated on total germination and total root length parameters). In contrast, the control seedlings were placed in the same system without the presence of *P. atriplicifolia* plant material.

2.2.1. Effects of VOCs on A. retroflexus plant growth and water status

The effects of VOCs on fresh weight (FW), dry weight (DW), and DW/FW ratio were determined at the end of the experiments on four seedlings before and after oven drying (60°C till constant weight was reached).

Leaf relative water content (RWC) evaluation was carried out following the method proposed by Araniti et al. (2017) and calculated for each replicate using the following formula:

$$\mathbf{RWC} = [(\mathbf{FW} - \mathbf{DW}) / (\mathbf{TW} - \mathbf{DW})] * \mathbf{100}$$

Where TW represents the turgid weight (TW).

Also, the leaf Ψπ was measured at the end of the experiment as previously described by Araniti et al. (2017) on four leaves per treatment (0 and 110 g cut plant material), using a cryoscopic osmometer (Osmomat 030, Gonatec) and expressing it as mOsmol/Kg.

2.2.2. Lipid peroxidation and membrane stability index

Lipid peroxidation, used to monitor the increase of malondialdehyde (MDA) in the sample, was determined on 100 mg of N_2 snap-frozen material. The supernatant absorbance was measured at 440, 532, and 600 nm, and the equivalents of MDA were calculated using the equations proposed by Hodges et al. (1999) and adjusted by Landi (2017).

The membrane stability index (MSI) was determined, using a WTW compact inoLab Cond Level 1 precision conductivity meter (Weilheim 2002, WTW GmbH & Co. KG, Germany), as reported by Sairam et al. (2005), with some modifications. Leaf discs (0.5 cm Ø) were transferred to 50 ml tubes filled with 10 ml of ultrapure water. Before measuring the electrical conductivity (C1), the samples were heated at 30°C for 30 minutes. Successively, the samples were heated at 100°C for 30 minutes and cooled in ice, and once at room temperature, the electric conductivity (C2) was newly measured. The following formula was used to calculate the MSI:

$$\mathbf{MSI}(\%) = (\mathbf{1} - \mathbf{C_1} / \mathbf{C_2}) * \mathbf{100}$$

2.2.3. GC-MS-driven untargeted metabolomics analysis on plant metabolism

The untargeted metabolomics analysis was carried out in *A. retroflexus* aerial tissues following the protocol of extraction and analysis proposed by Lisec et al. (2006), with some modifications.

After extraction and MSTFA derivatization, the samples spiked with ribitol as internal standard (0.2 mg/ml) were injected into the previously described GC-MS apparatus equipped with the same column (MEGA 5-MS).

The injector and source were set to 250°C and 260°C, respectively. Samples (1μl) were injected in splitless mode with a helium flow of 1ml/min. Chemical chromatographic separation was achieved using the following temperature ramp: isothermal 5 min at 70°C, followed by a 5°C/ min ramp to 350°C and a final 5 min heating at 330°C. Mass spectra were recorded in electron impact (EI) mode at 70 eV, scanned over the 40–600 m/z range. *n*-Alkane standards (C10–C40, all even), blank solvents, and qualitative controls (QC – control and treated pooled samples) were injected at scheduled intervals to monitor instrumental performance, facilitate tentative identification, and detect shifts in retention indices.

Chromatographic sample alignment, deconvolution, peak extraction, and annotation were carried out using the open-source software MS–DIAL *ver.* 4.48. Chemical annotation was achieved following the steps previously described for VOCs identification.

2.2.4. GC-MS analysis of the cuticular waxes

Cuticular wax extraction was achieved by immersing *A. retroflexus* plant leaves (six per replicate) for 30 seconds in 4 ml of *n*-hexane as previously described by Lavergne et al. (2018). The leaves were then derivatised with MSTFA in pyridine (30 min at 70 °C, shaking at 950 rpm).

Chemical composition and relative amount of extracted cuticular waxes were measured using the previously described GC-MS equipped with the same column. One microliter for each replicate was injected into the GC inlet S/SL, settled at 230°C, in splitless mode with a 1 ml min^{-1} flow rate of helium (99.9 % purity) as a carrier gas and a pre-column pressure of 112.9 kPa. The GC oven temperatures were set as follows: 3 min at 40°C, followed by a 5°C min-1 increment up to 230°C, followed by 40 min at 230°C. The mass spectrometer was operating in electron impact mode with an electron energy of 70 eV. The temperature of the ion sources and quadrupole was 200°C, and it was working in full scan mode, ranging from 40 to 600 amu.

2.2.5. GC/MS data analysis using MS-DIAL

All metabolomic data were aligned, deconvoluted, and the peak intensities extracted, using the open-source software MS-DIAL equipped with open-source publicly available EI spectral libraries as previously described by Misra et al. (2020).

For metabolite annotation and assignment of the EI-MS spectra, we followed the metabolomics standards initiative (MSI) guidelines for metabolite identification (Sumner et al., 2007). In particular, metabolites were annotated at level 2 (identification based on the spectral database) (Sumner et al., 2007).

2.2.6. Determination of lignification-related enzyme activity and total phenolic content

Polyphenol oxidase (PPO) activity was evaluated spectrophotometrically according to Siriphanich and Kader (1985), monitoring the rate of catechol oxidation over time. Phenylalanine ammonia-lyase (PAL) activity was assayed by adapting the procedure of D'Cunha et al. (1996), in which the formation of trans-cinnamic acid from L-phenylalanine is quantified. Lignin was isolated and quantified on isolated alcohol-insoluble cell wall material using the acetyl bromide extraction and spectrophotometric quantification method described by Foster et al. (2010). Total phenolic compounds were measured via the Folin–Ciocalteu colourimetric assay (Singleton and Rossi, 1965), with absorbance values interpolated against a gallic acid standard curve, and the concentrations were reported as milligrams of gallic acid equivalents per gram of fresh tissue (Lee et al., 2007).

2.3. Experimental design and statistical analysis

All measurements of the experiment were conducted using a completely randomized design with three replications. For the experiment on developed seedlings, each replication consisted of a pool of 10

plants.

Total germination index, germination speed, and total root length responses to different doses of plant material were analysed using a nonlinear regression model with a log-logistic function to calculate the ED_{50} values, as reported by Araniti et al. (2013b).

Metabolomic statistical analyses (untargeted metabolomics and cuticular waxes) were performed using the online, open-source software Metaboanalyst 5.0. Metabolite concentrations were checked for integrity, and missing values were replaced with a small positive value (half of the minimum positive number detected in the data).

Before performing univariate (t-tests – $P \leq 0.05$) and multivariate analysis, data were normalised for untargeted metabolomic analysis through the Internal standard (ribitol) process (MS-DIAL), whereas for cuticular wax analysis, through the MS-DIAL mTIC function (TIC of identified metabolites) and the dry weight of the leaf samples used for the analysis. The data were then logarithmically transformed (Log_{10}) and scaled using the "Pareto-Scaling" method. Cuticular wax normalised data were then analysed through Univariate t-test analysis ($P \leq 0.05$ and a False Discovery Rate - FDR ≤ 0.05). In contrast, the metabolomic analysis carried out on plant tissues was conducted using both univariate and multivariate methods. In particular, for multivariate analysis, the data were classified using unsupervised principal component analysis (PCA), and the variations in metabolites were presented as a heatmap. Successively, the data were further analysed through t-test ($P \leq 0.05$ and a FDR ≤ 0.05) and Fold Change (FC) using a FC cutoff of 1.5. Successively, the data were graphically represented using a Volcano plot. Next, to evaluate the possible biological impacts on the perturbed pathways, a "Pathway analysis" was carried out using the Metaboanalyst tool MetPa; *Arabidopsis thaliana* was used as a reference metabolome database. Finally, we calculated pairwise partial correlations among metabolites using the debiased sparse partial correlation (DSPC) method (betweenness filter cutoff = 1), which uncovers direct relationships between metabolite pairs while accounting for indirect links.

3. Results

3.1. Experiments on seeds and young seedlings

Perovskia atriplicifolia releases a terpene-rich volatile blend

The HS-SPME-GC-MS analysis of VOCs emitted by the living *P. atripicifolia* plant identified seventy volatiles, mainly belonging to the classes of monoterpenes and oxygenated terpenes, with smaller amounts of esters and furan derivatives. (Table 1). Among them, the monoterpene O-Cymene (33%) was the most relevant compound, followed by D-Carene (15 %), 4-(5-methyl-2-furanyl)-2-butanone (14 %), (E)-3,7-dimethyl-2,6-octadien-1-yl acetate (also known as geranyl acetate) (9.7 %), and α-Thujene (7.4 %). Together, these six compounds accounted for nearly 80 % of the volatile blend (Table 1).

3.2. Perovskia atriplicifolia volatiles inhibit germination and root growth of Amaranthus retroflexus

The *in vitro* bioassays on seed germination showed that the VOCs emitted by the test species significantly affected both parameters. In particular, G_T% was notably reduced by 40 % and 62 %, at doses of 100 g and 200 g, respectively. In addition, the dose-response curve fitting through non-linear regression highlighted an ED_{50} of 140 g (Fig. 1). Also, the parameter S was significantly inhibited by the VOCs already at low concentrations (9% of inhibition at doses of 50 g), reaching inhibition values of 61 % (100 g) and 74 % (200 g) and ED_{50} value of 96.1 g (Fig. 1).

Similarly to germination, the total root length was inhibited only at the two highest concentrations assayed, pointing out inhibition values of 63 % (100 g) and 74 % (200 g) and an ED_{50} value of 91.5 g (Fig. 1).

Table 1
HS-SPME-GC-MS-based identification of VOCs released by *Perovskia atriplicifolia*.

Name	RT(min)	KI	RAP %	Class
Methyl-2-butenal (3-)	5.9049	763.3214	0.003381	Aldehyde
Hexanal -b	6.968367	800.8804	0.003481	Aldehyde
Thujene (alpha-)	11.3459	916.3826	7.510518	Monoterpenes
Pinene (alpha-)	11.90237	931.0651	0.015492	Monoterpenes
Sabinene	13.21315	965.6504	0.777326	Monoterpenes
Myrcene	13.9716	985.6623	0.41556	Monoterpenes
Carene (delta-3-)	15.05155	1011.418	15.4946	Monoterpenes
Cymene (ortho-)	16.32523	1038.524	33.61727	Monoterpenes
Cineole (1,8-)	16.49012	1042.033	8.009146	Monoterpenes
Ocimene (e-beta-)	16.56018	1043.524	1.016271	Monoterpenes
Terpinene (gamma-)	16.8817	1050.366	0.106494	Monoterpenes
Sabinene hydrate (cis-)	17.89158	1071.857	0.607406	Monoterpenes
Terpinolene	18.79018	1090.981	1.296701	Monoterpenes
Menth-2-en-1-ol (cis-para-)	19.10345	1097.647	0.01866	Monoterpenic alcohol
Linalool	19.24772	1100.718	0.044299	Monoterpenic alcohol
Ocimene (allo-)	20.71927	1132.034	0.018655	Monoterpenes
4-(5-methyl-2-furanyl)-2-butanone	21.99707	1159.227	14.46933	Heteroaromatic ketone
Methyl phenylacetate	23.0152	1180.894	0.000741	Aromatic ester
Hexenyl butanoate (3z-)	23.39853	1189.052	0.011249	Aliphatic ester
Sabinene hydrate acetate (cis-)	23.52632	1191.771	0.232863	Monoterpenes acetate
Methyl salicylate	23.67058	1194.841	0.005255	Aromatic ester
Bornyl formate	25.1545	1229.999	0.089286	Monoterpenoid ester
Hexenyl 3-methyl butanoate (3z-)	25.46365	1237.469	0.007781	Aliphatic ester
Cyclocitral (beta-)	25.64913	1241.951	0.00588	Monoterpenes
(1r)-1,7,7-trimethylbicyclo (2.2.1)heptan-2-one	26.08195	1252.409	0.002091	Monoterpenoid ketone
Alpha-terpinene	26.5601	1263.963	0.496607	Monoterpenes
Thujanol acetate (3-)	27.9121	1296.632	2.71709	Monoterpenes acetate
Verbenone	28.42735	1309.082	0.003158	Monoterpenes
5-methyl-2-(1-methylethyl)-phenol	28.60047	1313.265	0.110766	Monoterpenoid phenol
Isopulegyl acetate (equatorial)	29.16518	1326.91	0.020258	Monoterpenes acetate
Dihydrocarvenyl acetate(equatorial)	29.89065	1344.44	0.040349	Monoterpenes acetate
4-terpinyl acetate	30.49245	1358.982	1.714789	Monoterpenes acetate
Neryl acetate	31.05303	1372.527	0.004771	Monoterpenes acetate
Cubebene (alpha-)	31.16845	1375.316	0.031169	Sesquiterpenes
Bornyl propionate	31.3828	1380.495	0.002989	Monoterpenoid ester
Neryl formate	31.7579	1389.559	0.006619	Monoterpenoid ester
Caryophyllene (z-)	32.47925	1410.545	0.069777	Sesquiterpenes
Guaiadiene (6,9-)	33.14288	1434.739	0.088213	Sesquiterpenes
(E)-3,7-dimethyl-2,6-octadien-1-yl acetate	34.07032	1468.55	9.803687	Monoterpenoid ester
Longifolene	34.16925	1472.156	0.184208	Sesquiterpenes
Iso-longifolene	34.49077	1483.878	0.010242	Sesquiterpenes
Δ-cadinene	35.0225	1503.263	0.007551	Sesquiterpenes
Alloakumadendrene	35.12967	1507.17	0.237668	Sesquiterpenes
α-cubebene	35.2657	1512.129	0.026217	Sesquiterpenes
α-gurjunene	35.81392	1532.115	0.033181	Sesquiterpenes
Gamma-muurolene	35.9046	1535.421	0.139875	Sesquiterpenes
Cadinene (delta-)	36.27145	1548.795	0.039455	Sesquiterpenes
α-Guaiene	36.36627	1552.252	0.260384	Sesquiterpenes
Δ-Guaiene	36.4487	1555.257	0.006434	Sesquiterpenes
β-Selinene	36.89387	1571.486	0.008968	Sesquiterpenes
Alpha-selinene	37.236	1583.959	0.001193	Sesquiterpenes
Epoxyvulgarone a	37.38027	1589.219	0.123429	Monoterpenoid ester

(*continued on next page*)

Table 1 (*continued*)

Name	RT(min)	KI	RAP %	Class
(E)-3,7-dimethyl-2,6-octadien-1-yl isobutyrate	37.743	1603.541	0.006481	Monoterpenoid ester
Germacrene-d	38.04803	1619.664	0.00148	Sesquiterpenes
Elemol	39.63498	1703.54	0.003535	Sesquiterpenes
Heptadecane	39.66796	1705.284	0.001685	Alkane
Tridecanal	39.97298	1721.405	0.001194	Alkane
3-isopropyl-6,10-dimethylundecane-2-ol	41.42805	1798.311	0.00088	Sesquiterpenoid alcohol

RT: retention time. RI: retention index; RAP% (Relative area percentage, peak area relative to total peak area of the identified peaks %). N=3.

3.3. ED_{50}-based VOCs exposure was selected for established seedling assays

Since the successive experiments were carried out on established seedlings, which could be less sensitive to VOCs phytotoxicity, and noting that there are no vast differences between the ED_{50} calculated on germination and total root length, we decided to use an amount of *P. atripicifolia* plant material equal to the average of the ED_{50} values from G_T% and total root length, rounded up. Therefore, all subsequent experiments used 120 g of *P. atripicifolia* plant material, which was replaced daily throughout the experiments.

3.4. VOCs exposure impairs growth and water status in Amaranthus retroflexus

Exposure of *Amaranthus retroflexus* to the volatile compounds released by fresh material of *Piararska atripicifolia* significantly altered plant growth and physiological parameters. Fresh weight (FW) decreased from approximately 2.15 g in control plants to 1.80 g in VOCs-exposed plants (-16%; Fig. 2). In contrast, dry weight (DW) was only slightly affected, showing a nonsignificant decrease of ~5% (0.20 g in controls vs. 0.19 g in treated plants) (Fig. 2). The DW/FW ratio, however, was significantly increased under VOCs exposure, rising from ~0.095 in control plants to ~0.11 in treated ones, indicating a stimulation of approximately 16% (Fig. 2). Relative water content (RWC) was markedly reduced, with values declining from ~77% in control plants to ~67% in exposed plants (120 g), representing an inhibition of around 13% (Fig. 2). Finally, leaf osmotic potential (Ψπ), expressed as osmolality, increased significantly following exposure to VOCs. Control plants reached values of about 570 mOsmol/kg, while exposed plants (120 g) exhibited values close to 660 mOsmol/kg, corresponding to an increase of nearly 16% (Fig. 2).

3.5. VOCs enhance phenylpropanoid activity and lignin accumulation

Exposure of *Amaranthus retroflexus* plants to volatile compounds released by 120 g of fresh *Pierarska atripicifolia* material led to differential modulation of several physiological and biochemical parameters.

The membrane stability index (MSI) was not significantly affected by

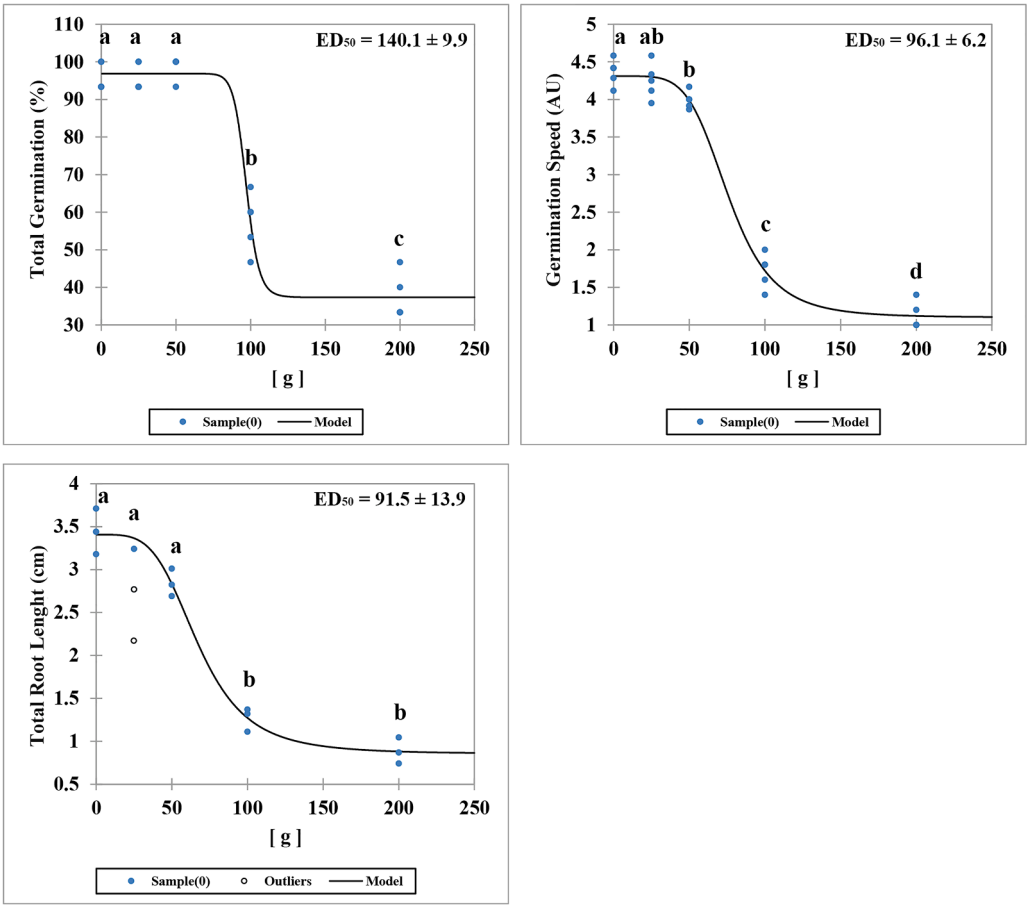

Fig. 1. Effects of VOCs released by different doses of *P. atriplicifolia* aerial parts (0 g, 25 g, 50 g, 100 g, and 200 g) on total germination index (G_T% %), speed of germination (S expressed as arbitrary units – AU) and total root length (TRL). Data were statistically analysed through one-way ANOVA using Tukey's test as post hoc ($P \leq 0.05$). Different letters along the curves indicate significant differences among treatments. The dose-response curves were fitted through non-linear regression using equation (1) to calculate the ED_{50}. All the dose-response curves pointed out a significance level of $P \leq 0.001$. N = 3.

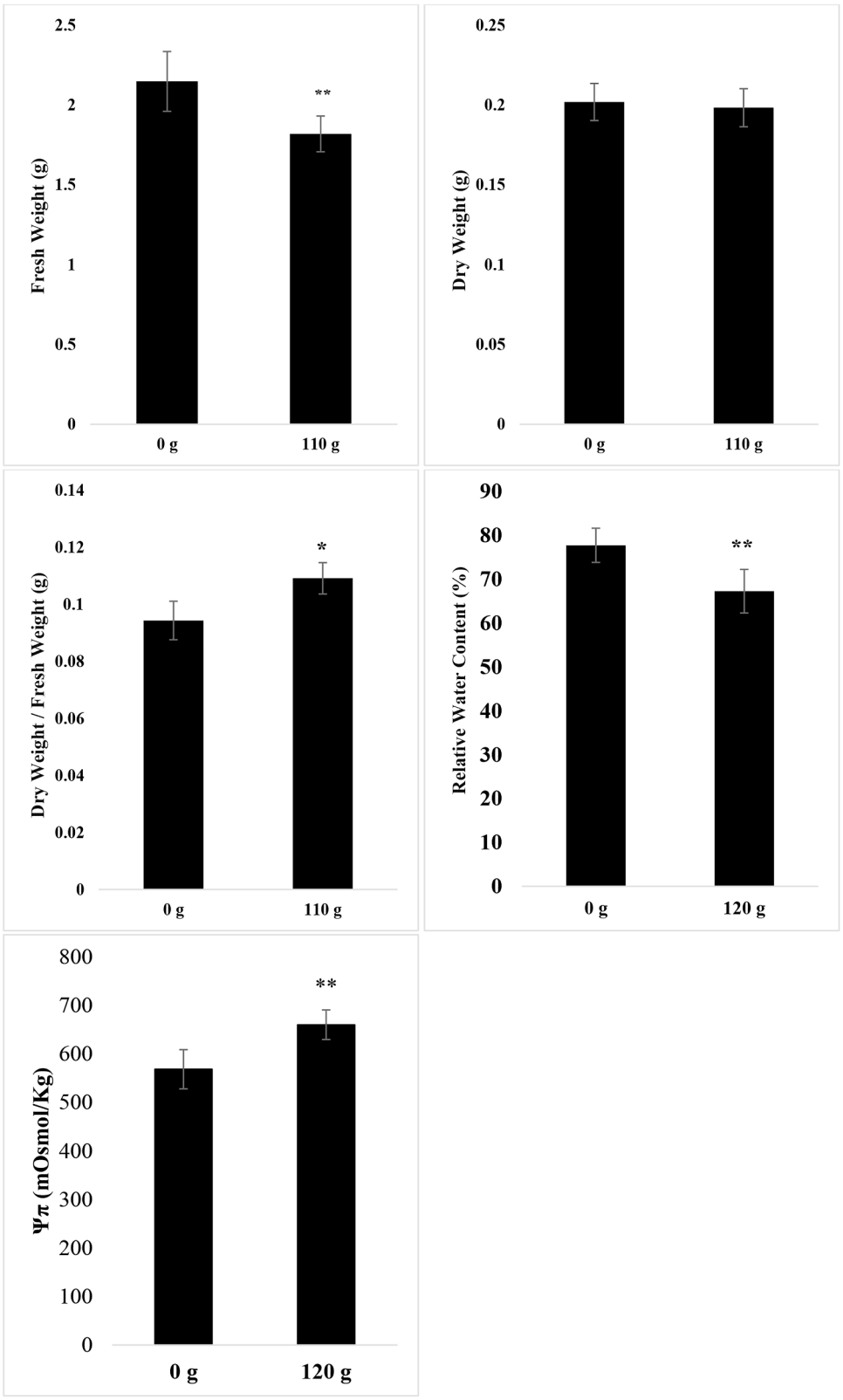

Fig. 2. Effects of VOCs produced by 110 g of *P. atriplicifolia* aerial parts on several plant growth and water status parameters. Fresh weight (FW), dry weight (DW), DW/FW ratio, relative water content (RWC), and osmotic potential (Ψπ, expressed as osmolality). Data are expressed as mean ± SD. Data were statistically analysed through the Student's test, and * ($P \leq 0.05$),**($P \leq 0.01$), or *** ($P \leq 0.001$) indicate statistical differences between treatments. N = 3.

VOC exposure (Fig. 3). Likewise, lipid peroxidation, expressed as malondialdehyde equivalents (MDA), showed no significant differences between control and treated plants (Fig. 3), indicating that oxidative stress levels were not influenced by VOCs.In contrast, significant responses were observed in the phenylpropanoid metabolism. Phenylalanine ammonia-lyase (PAL) activity increased markedly, from about 11.5 to 17.5 U mg^{-1} protein, corresponding to an enhancement of ~52% (***$p < 0.001$) (Fig. 3). Polyphenol oxidase (PPO) activity also rose significantly, from ~0.25 to ~0.70 U mg^{-1} protein, representing a ~180% enhancement (**$p < 0.01$) (Fig. 3).

Consistently, the total phenolic content increased from ~2.1 to ~3.3 μmol g^{-1} DW, corresponding to an enhancement of ~57% (***$p < 0.001$). Likewise, lignin accumulation showed a significant rise, from ~90 to ~145 μg mg^{-1} cell wall, i.e. ~61% stimulation (***$p < 0.001$) (Fig. 3).

3.6. VOCs remodel cuticular wax composition

Given the observed alterations in water status and osmotic potential, we next investigated whether VOC exposure affected cuticular composition. The plant cuticle is a primary barrier controlling non-stomatal water loss and undergoes compositional adjustments under stress. Therefore, changes in wax and fatty acid profiles could reflect structural adaptations aimed at stabilising leaf water balance under volatile exposure.

Metabolomic analysis of the leaf cuticle, combined with chemical characterization, led to the identification of 67 compounds belonging to several chemical classes, including alkanes, fatty acids, fatty alcohols, and sterols. Full details on retention time, retention index, quantified mass, chemical formula, and peak intensities are provided in Supplementary Table S1. Peak intensities of all identified metabolites were analysed in MetaboAnalyst using a univariate *t*-test, which revealed 41 compounds significantly affected by VOC exposure (Table 2). Specifically, four 1-monoacylglycerols were reduced considerably, whereas one acyclic diterpenoid and nine alkanes were increased. The treatment also promoted the accumulation of one cyclic ketone, two fatty alcohols, two fatty alcohol esters, four long-chain fatty alcohols (three increased and one decreased), quinic acid, an important precursor for both cuticle-associated metabolites and the shikimate pathway, one sterol precursor, four sterols (two increased and two decreased), one triterpenoid, one wax monoester, and two very long-chain fatty acids (one increased and one decreased). In contrast, two unsaturated aliphatic hydrocarbons and one sugar alcohol were reduced (Table 2; Supplementary Table S1).

3.7. VOCs reprogram primary and secondary metabolism

The coordinated alterations in water status, phenylpropanoid enzyme activity, lignin accumulation, and cuticular wax composition suggest that VOC exposure induces a broader metabolic reprogramming in *A. retroflexus*. To obtain a system-level overview of these responses and identify the metabolic pathways underlying the observed physiological and structural changes, we performed an untargeted GC–MS metabolomic analysis.

The GC-MS-driven metabolomic analysis on *A. retroflexus* leaves exposed to *P. atripicifolia* volatiles allowed more than 2200 features to be extracted. After excluding unknown compounds and false annotations, only 174 metabolites, characterised by a total score similarity higher than 80 %, were annotated putatively (Supplementary Table S2). An overview of the metabolic variation induced by VOC exposure was first obtained by Principal Component Analysis (PCA). The first two components explained 76.9% of the total variance, with PC1 alone accounting for 63.6% (Fig. 4a). The score plot showed a clear separation between control and treated plants, with tight clustering of replicates within each group, indicating that VOC exposure produced a consistent metabolic reprogramming (Fig. 4a). The loading plots revealed that phenolic acids such as ferulic, p-coumaric, caffeic, and sinapic acids, together with their precursors shikimic and quinic acids, as well as amino acids including phenylalanine, tyrosine, and proline, contributed most strongly to the separation of treated samples along PC1 (Supplementary Table S2). In contrast, control plants exhibited higher levels of carbohydrates and sugar alcohols, including raffinose, melezitose, glucose, mannitol, and galacturonic acid, which loaded negatively on PC1 (Supplementary Table S2). This indicates that the metabolic signature of VOC-exposed plants was dominated by the accumulation of phenolic intermediates and amino acids, paralleled by a reduction in soluble sugars and osmoprotectants (Supplementary Table S2).

Univariate statistical analysis provided a more detailed assessment of these changes (Fig. 4b and Supplementary Table S2). Using a fold change cut-off of 1.5 and a *p*-value threshold of 0.05, forty-one metabolites were identified as significantly altered by VOC exposure. Among the most striking changes, several key intermediates of the shikimate–-phenylpropanoid pathway were strongly accumulated (Fig. 4b and Fig. 5). Sinapic acid showed the most pronounced increase, while ferulic acid, p-coumaric acid and caffeic acid also rose significantly, indicating a substantial activation of phenolic acid biosynthesis (Fig. 4b and Fig. 5). In addition, the aromatic amino acids phenylalanine and tyrosine, both direct precursors of this pathway, were significantly accumulated (Fig. 4b and Fig. 5). Interestingly, one caffeic acid derivative was instead strongly reduced, suggesting a selective redirection of metabolic fluxes within this pathway (Fig. 4b).

Alongside these phenylpropanoid intermediates, several other amino acids and nitrogen-related metabolites were strongly increased, including cysteine, glutamic acid, arginine, and β-cyano-L-alanine, all of which are associated with stress adaptation and nitrogen redistribution (Fig. 4b). Proline and β-alanine also accumulated, reinforcing the role of nitrogen metabolism in the response to VOC exposure. In contrast, multiple soluble carbohydrates and polyols were markedly depleted (Fig. 4b). Mannitol, raffinose, melezitose, glucose, and galacturonic acid all showed strong reductions in treated plants, indicating a loss of osmolytes and energy reserves. Additional significant increases were observed for compounds such as N-acetyl-galactosamine, sarcosine, dehydroascorbic acid, and diglycerol, pointing to a broader reconfiguration of carbohydrate, amino sugar, and redox-related pathways (Fig. 4b).

Pathway enrichment analysis confirmed that phenylalanine metabolism and phenylpropanoid biosynthesis were among the significantly affected pathways (Table 3). In addition, cysteine and methionine metabolism was altered considerably, suggesting enhanced flux toward glutathione and S-adenosylmethionine, which are essential for redox balance and methylation reactions within the phenylpropanoid pathway (Table 3). Arginine and proline metabolism was also perturbed, reflecting the accumulation of proline and other intermediates linked to stress tolerance (Table 3). Changes in pantothenate and CoA biosynthesis pointed to increased demand for activated CoA intermediates in monolignol biosynthesis. Other pathways significantly affected included cyanoamino acid metabolism, thiamine metabolism, and sulfur metabolism, indicating that the impact of VOC exposure extended beyond secondary metabolism into primary metabolic routes linked to nitrogen and sulfur homeostasis (Table 3).

Finally, Debiased Sparse Partial Correlation (DSPC) network analysis showed that the metabolic restructuring involved not only changes in abundance but also in connectivity (Table 4 and Fig. 6). Several amino acids emerged as highly connected hubs: arginine (Degree = 17, Betweenness = 74.67), cysteine (Degree = 14, Betweenness = 85.57), and glutamic acid (Degree = 13, Betweenness = 29.13) established strong local connections linking primary nitrogen metabolism with secondary metabolism (Table 4 and Fig. 6). Pyroglutamic acid (Degree = 11, Betweenness = 73.88) also occupied a central position, bridging distinct modules. Despite its strong depletion, mannitol (Degree = 7, Betweenness = 125.71) displayed the highest betweenness, indicating that its reduction had a disproportionately large impact on the redistribution of carbon fluxes across the network (Table 4 and Fig. 6).

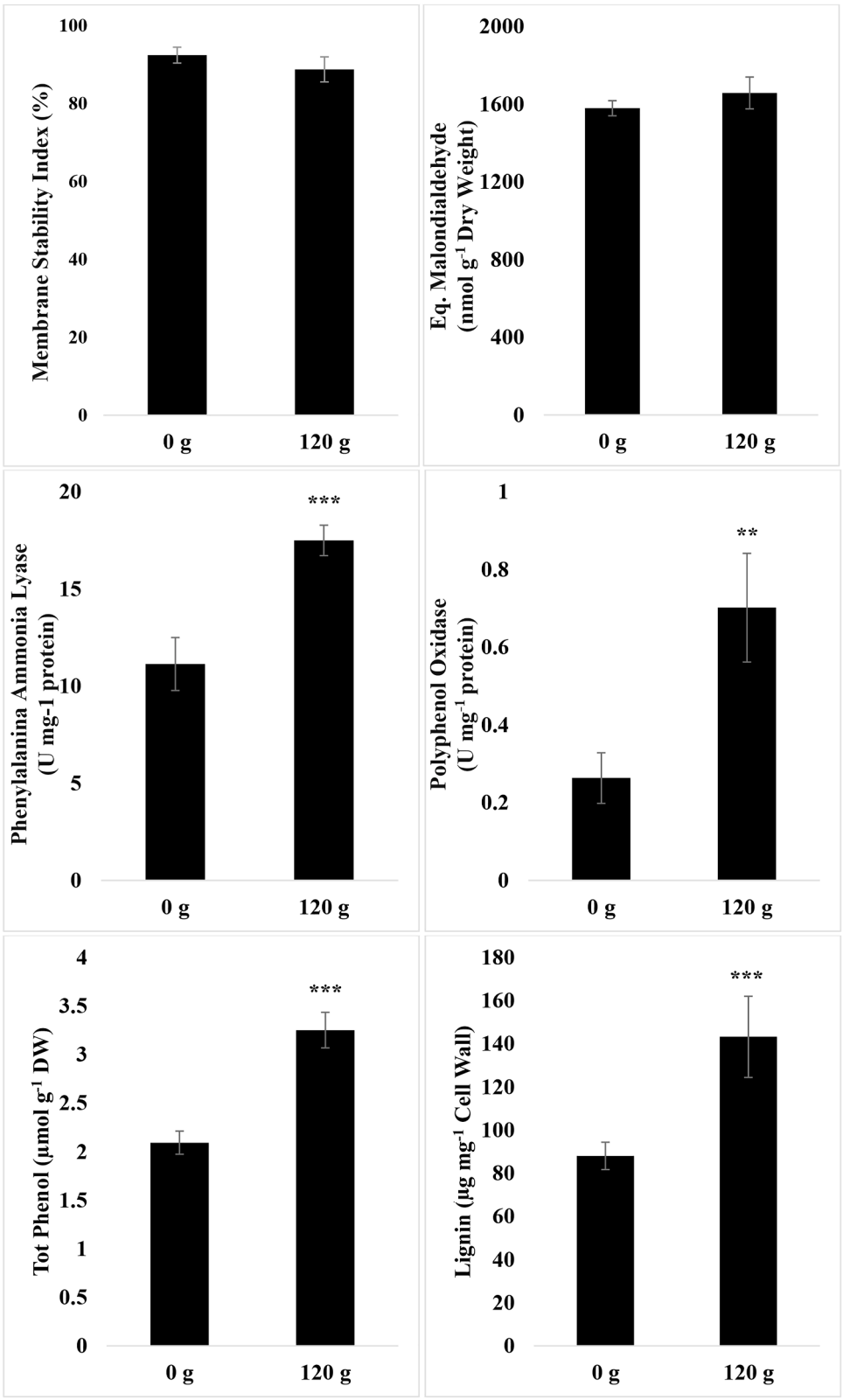

Fig. 3. Effects of VOCs produced by 110 g of *P. atriplicifolia* aerial parts on the membrane stability index (MSI), lipid peroxidation (MDA), Phenylalanine ammonia-lyase (PAL) and Polyphenol oxidase (PPO) activity, total phenolic and lignin content. Data are expressed as mean ± SD. Data were statistically analysed through the Student's test, and * ($P \leq 0.05$),** ($P \leq 0.01$), or *** ($P \leq 0.001$) indicate statistical differences between treatments. N = 3.

Table 2
Effects of *P. atripicifolia* VOCs on the cuticular wax composition of *A. retroflexus*.

Metabolite	t.stat (treated vs control)	p.value	FDR	Class
Monostearin	101.59	5.63E-08	3.77E-06	1-monoacylglycerols
Monopalmitin	70.455	2.43E-07	5.43E-06	
Monoolein	44.336	1.55E-06	1.61E-05	
Monomyristin	4.2891	0.012756	0.02374	
Phytol	**-18.366**	5.17E-05	0.000231	Acyclic diterpenoids
Squalene	**-59.359**	4.82E-07	7.42E-06	Triterpenoids
Dodecane (C12)	**-6.1204**	0.00361	0.008061	Alkanes
Tridecane (C13)	**-3.7724**	0.019565	0.032771	
Tetradecane (C14)	**-5.8824**	0.004174	0.008767	
Hexadecane (C16)	**-30.937**	6.50E-06	3.63E-05	
Heptadecane (C17)	**-9.6526**	0.000644	0.001962	
Nonadecane (C19)	**-13.379**	0.00018	0.000672	
Pentacosane (C25)	**-32.949**	5.06E-06	3.08E-05	
Nonacosane (C29)	**-36.151**	3.50E-06	2.34E-05	
Hentriacontane (C31)	**-42.199**	1.89E-06	1.61E-05	
1-Hexadecene	5.0495	0.007234	0.014254	Unsaturated aliphatic hydrocarbons
Tetradecene (1-)	3.4167	0.026862	0.043896	
5-Cyclohexadecenone	**-7.0439**	0.002141	0.00544	Cyclic ketones
Methyl linoleate	57.353	5.53E-07	7.42E-06	Fatty acid methyl esters
Methylhexadecanoate	12.518	0.000234	0.000785	
Suberic acid	**-9.1096**	0.000805	0.002346	Medium-chain fatty acids
Palmitic acid	6.2603	0.003321	0.007673	Long-chain fatty acids
Linoleic acid	4.03	0.015733	0.027029	
Lignoceric acid	**-41.994**	1.92E-06	1.61E-05	Very long-chain fatty acids
Octacosanoic acid	12.746	0.000218	0.00077	
Octadecanol	**-4.9275**	0.007887	0.015098	Fatty alcohol
1-Undecanol	**-4.1412**	0.014362	0.025323	
Undecyl acetate	**-8.303**	0.001149	0.003208	Fatty alcohol esters
(Z,Z)-7,11-Hexadecadienyl acetate	**-5.8774**	0.004187	0.008767	
Tetradecanol	6.9998	0.002192	0.00544	Long-chain fatty alcohols
Pentadecanol (n-)	**-6.7418**	0.002523	0.006037	
(Z)-2-Tridecen-1-ol	**-5.6765**	0.004752	0.009649	
1-Hexadecanol	**-4.1997**	0.013699	0.024806	
Hexitol	**-37.056**	3.17E-06	2.34E-05	Sugar alcohols
Quinic acid	**-74.222**	1.97E-07	5.43E-06	Quinic acids and derivatives
Obtusifoliol	**-10.383**	0.000486	0.00155	Sterol precursor
Beta-Sitosterol	26.168	1.27E-05	6.53E-05	Sterols
Campesterol	23.714	1.88E-05	8.97E-05	
alpha-Tocopherol	**-16.414**	8.06E-05	0.000338	
Lanosterol	**-14.414**	0.000135	0.000531	
Lauryl stearate	**-7.9919**	0.001329	0.003562	Wax monoesters

T-test analysis ($P \leq 0.05$) of the cuticular waxes characterised in *A. retroflexus* control and plants treated with *P. atriplicifolia VOCs*. t.stat, characterised by a positive value, indicates reduced chemical content in treated plants, whereas a t.stat negative value indicates an accumulation (bold fonts). The False Discovery Rate (FDR) test validated the P value, considering as altered all those metabolites characterised by a *P* value and an $FDR \leq 0.05$.

Among phenolic metabolites, sinapic acid (Degree = 4, Betweenness = 49.86) emerged as a key bridging node between primary and secondary metabolism, underscoring its role in channelling resources toward syringyl lignin biosynthesis (Table 4 and Fig. 6). Together, these patterns show that VOC exposure reorganised the metabolic network by increasing the centrality of amino acids and phenolic intermediates while weakening the role of sugar alcohols as connectors.

4. Discussion

Exposure of *A. retroflexus* to volatiles emitted by fresh *P. atriplicifolia* tissue resulted in a set of changes characteristic of volatile-mediated allelopathy (Xie et al., 2021): at first, its early growth and water balance were reduced, and later its metabolism shifted toward stress defence and strengthening of the cell wall through phenylpropanoid compounds. In our assays, the volatile treatment reduced total germination and slowed its progression, while also suppressing total root length. This aligns closely with the well-documented capacity of plant terpenoid volatiles to inhibit germination and root elongation in receiver species such as *Lactuca sativa, Lolium multiflorum, Trifolium subterraneum*, and *Plantago lanceolata*, among others (Araniti et al., 2017; Souza-Alonso et al., 2018; Silva et al., 2014). Classic and more recent studies using single constituents and/or natural mixtures, especially terpenoids such as 1,8-cineole, demonstrate dose-dependent inhibition of germination, mitosis in root apical meristems, and root extension, thereby reproducing the directional pattern observed in *A. retroflexus* (Verdeguer et al., 2020; Araniti et al., 2013a). Within the experiment on well-developed seedlings, early growth alterations co-occurred, indicating changes in leaf water relations, shifts in fresh mass, relative water content, and osmotic potential. These changes were accompanied by increased induction of polyphenol oxidase and phenylalanine ammonia-lyase activities, accompanied by higher total phenolics and lignin. Taken together, these physiological changes outline a stress syndrome similar to that already observed in other species after exposure to biologically active volatiles (Araniti et al., 2017; Santonja et al., 2019; Schulz et al., 2007). The volatile profile of *P. atriplicifolia* provides a plausible chemical basis for the observed bioactivity. The dominant compounds identified in *P. atriplicifolia*, including o-cymene, δ-3-carene and 1,8-cineole, are monoterpenes typically synthesized via the plastidial methylerythritol phosphate (MEP) pathway. Consistent with the volatile profiles reported for many Lamiaceae species, headspace analysis revealed a blend largely dominated by mono- and sesquiterpenes, several of which are known to impair germination and root growth in receiver plants (Verdeguer et al., 2020). Although oxygenated monoterpenes typically exhibit strong phytotoxicity, mixtures often act synergistically, strongly increasing the phytotoxicity of the single compounds (Asplund, 1969; Araniti et al., 2013a; Martino et al., 2010; Werrie et al., 2020). Mechanistically,

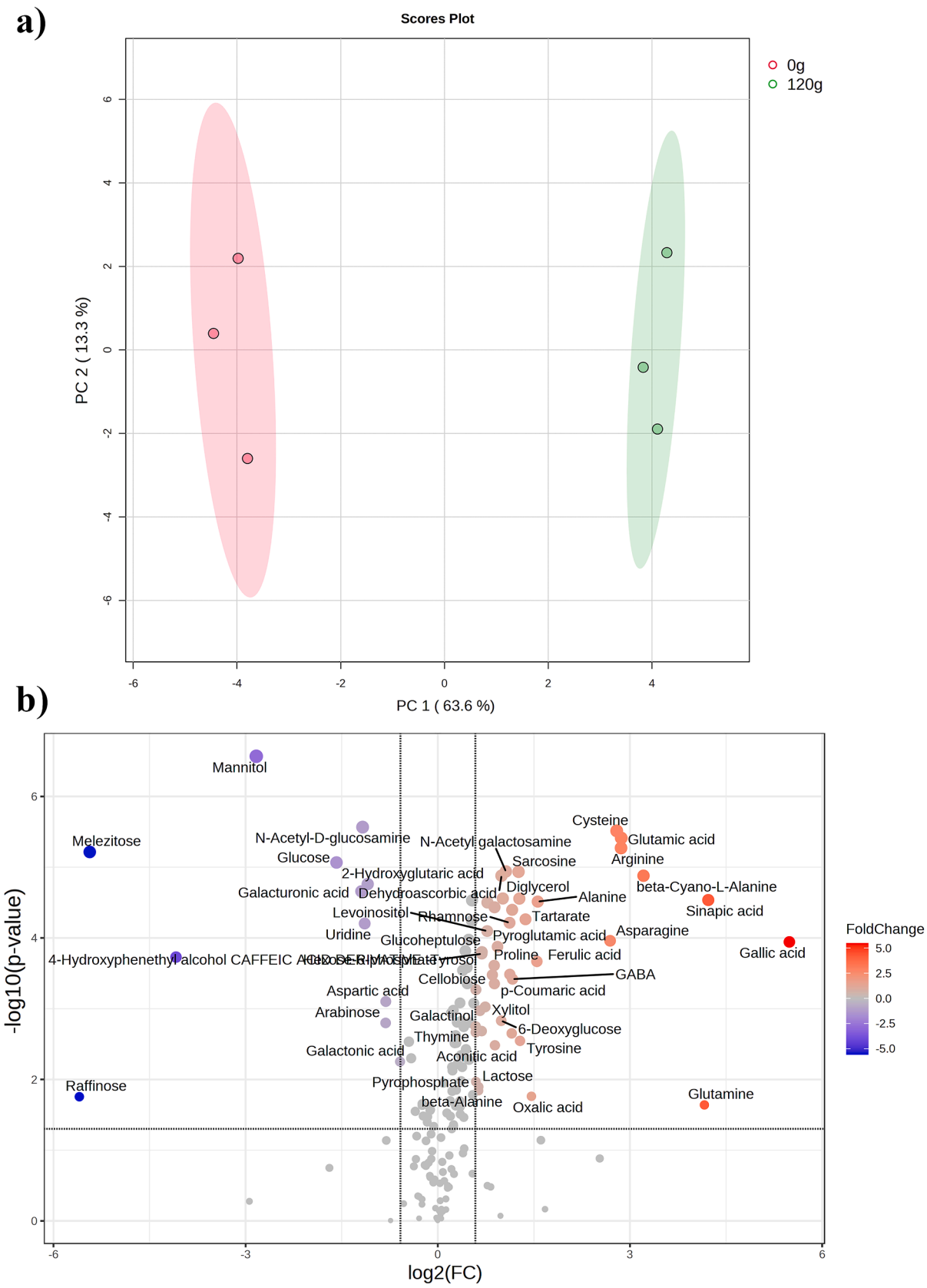

Fig. 4. Effects of *P. atripicifolia* volatiles on *A. retroflexus* metabolome. a) Score-plot of the Principal component; b) Volcano plot built using the metabolites with a fold-change $\geq$ 1.5 and a $P \leq 0.05$. N=3.

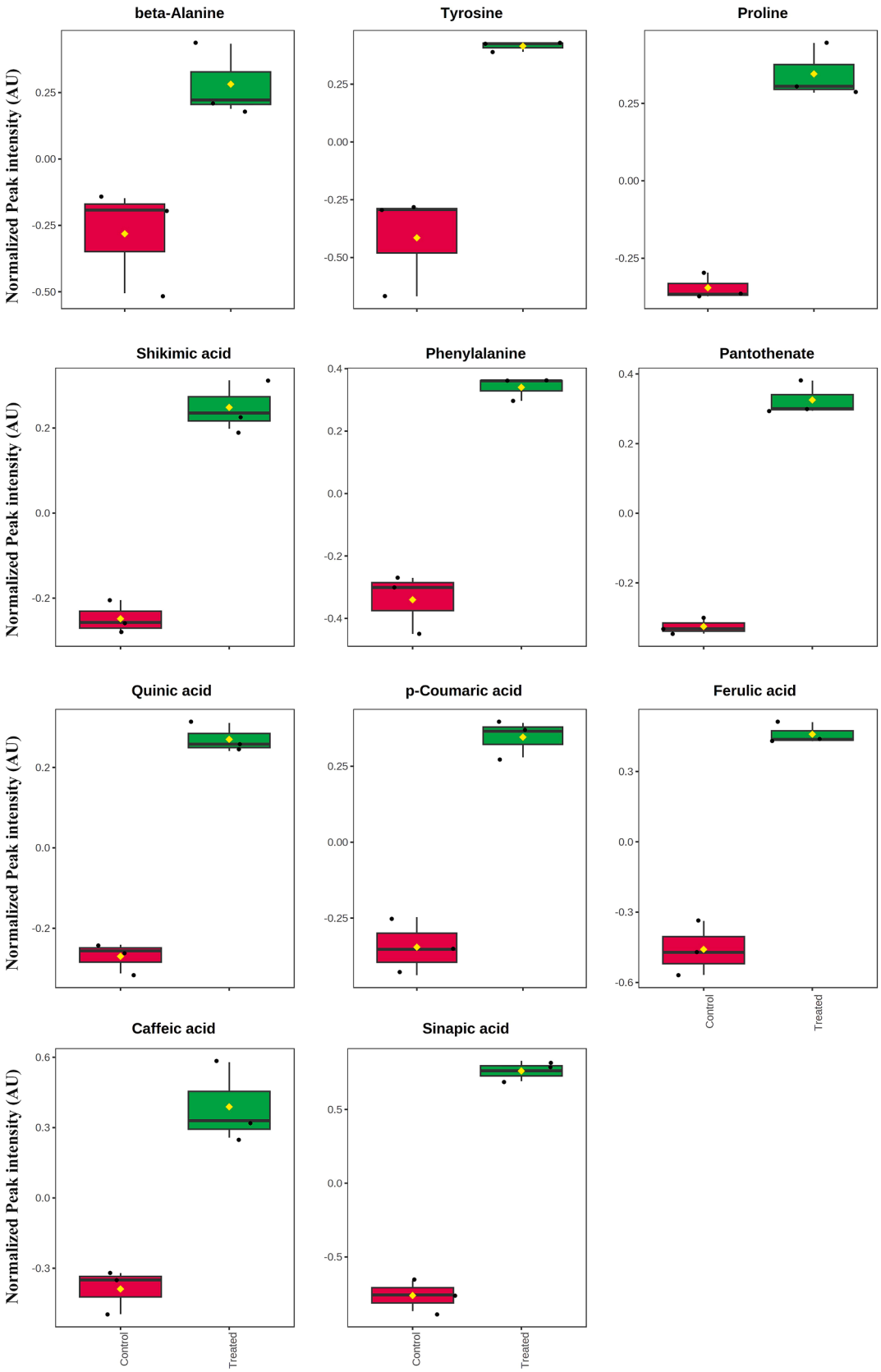

Fig. 5. Box plot of the main metabolites, extracted from Fig. 4, involved in lignin biosynthesis. N=3.

Table 3
Pathways analysis (enrichment+topology analysis) of *A. retroflexus* plants exposed to *P. atripicifolia* volatiles.

Pathways	Total Cmpd	Hits	Raw p	FDR	Impact
Biosynthesis of secondary metabolites - unclassified	5	1	0.00044337	0.001308	1
Alanine aspartate and glutamate metabolism	22	9	0.0011148	0.0025297	0.84532
Isoquinoline alkaloid biosynthesis	6	1	0.0028479	0.0050917	0.5
Glutathione metabolism	26	8	5.02E-05	0.00024726	0.4923
Phenylalanine metabolism	11	1	0.00033262	0.0010329	0.47059
Glyoxylate and dicarboxylate metabolism	29	10	0.014906	0.021451	0.38134
Cyanoamino acid metabolism	29	7	4.45E-06	6.57E-05	0.35593
Glycolysis / Gluconeogenesis	26	6	9.55E-05	0.00037546	0.35011
Arginine and proline metabolism	34	5	2.17E-05	0.00016002	0.32738
beta-Alanine metabolism	18	5	0.00028851	0.00094566	0.3254
Starch and sucrose metabolism	22	5	5.31E-05	0.00024726	0.32054
Galactose metabolism	27	7	0.0081313	0.012642	0.28841
Pantothenate and CoA biosynthesis	23	7	3.59E-06	6.57E-05	0.24406
Carbon fixation in photosynthetic organisms	21	7	0.0030803	0.0053453	0.21661
Arginine biosynthesis	18	6	0.00090488	0.0022245	0.20098
Butanoate metabolism	17	5	3.28E-05	0.00019335	0.13636
Glycerophospholipid metabolism	37	3	0.0050672	0.0085419	0.13525
Pyrimidine metabolism	38	6	0.0081424	0.012642	0.11868
Phenylpropanoid biosynthesis	46	5	0.0012357	0.0026038	0.11173
Tyrosine metabolism	16	2	0.0012148	0.0026038	0.10811
Inositol phosphate metabolism	28	4	2.09E-05	0.00016002	0.10251
Phenylalanine tyrosine and tryptophan biosynthesis	22	4	0.00080008	0.0020524	0.1016
Sulfur metabolism	15	2	1.86E-05	0.00016002	0.09392
Thiamine metabolism	22	5	5.90E-06	6.96E-05	0.06358
Cysteine and methionine metabolism	46	4	5.69E-07	3.36E-05	0.06036
Phosphatidylinositol signaling system	26	2	0.0014133	0.0028754	0.03285
Purine metabolism	63	4	0.017577	0.024691	0.01545
Ubiquinone and other terpenoid-quinone biosynthesis	38	2	0.00054131	0.0015208	0.00097

Total Cmpd: the total number of compounds in the pathway; **Hits:** the matched number from the uploaded data; ***P* value:** the original *P* value calculated from the enrichment analysis; **FDR:** false discovery rate for verifying that features called significant (with a *P* value $\leq$ 0.05) are truly null; **Impact:** the pathway impact value calculated from pathway topology analysis; //: not significantly impacted pathways. N = 3.

monoterpenes can depolarize plant plasma membranes and perturb membrane-associated processes (Maffei et al., 2001), trigger reactive oxygen species formation and lipid peroxidation in roots (Singh et al., 2006), and repress cell-cycle progression in meristems (Yoshimura et al., 2011; Nishida et al., 2005). In our experiment, although the effects on seedling establishment were consistent with previous reports, exposure of well-developed seedlings to VOCs did not cause any apparent reactive oxygen species-mediated damage to leaf membranes, as indicated by unchanged membrane stability index and lipid peroxidation parameters.

Table 4
DSPC network analysis carried out on the metabolites putatively annotated in *A. retroflexus* plants exposed to *P. atripicifolia* volatiles. The degree of node and betweenness of the interrelationships were calculated on the annotated metabolites in control and treated plants.

Label	Degree	Betweenness
Diglycerol	18	49.14
Arginine	17	74.67
Quinic acid	15	17.41
Cysteine	14	85.57
β-Cyano-L-Alanine	14	41.21
Rhamnose	14	25.67
Glucose 6-phosphate	14	21.84
Sarcosine	14	11.07
Glutamic acid	13	29.13
Isohexonic acid	13	11.9
Pyroglutamic acid	11	73.88
Fructose 6-phosphate	10	1.59
Pantothenate	9	0.66
Levoinositol	8	1.43
Glucoheptulose	8	1.42
Mannitol	7	125.71
Asparagine	7	7.65
Alanine	7	5.74
Hexose-6-phosphate	7	1
Melezitose	6	9.14
Iditol	6	0.71
2-Hydroxyglutaric acid	5	6.32
Sinapic acid	4	49.86
Mannose	4	7.27
Phenylalanine	4	5.5
Glucose	3	32.61
Dehydroascorbic acid	3	26.02
DL-2,3-Diaminopropionic acid	3	10.04
phytosphingosine	3	4.54
Erythronic acid lactone	3	0.95
Galactose	3	0.33
Arabinose	2	32
Ferulic acid	2	0
Ribonic acid	1	0

The response of plants to cope with water-balance alterations appears to be partially explained by cuticle remodelling. Our targeted analysis of cuticle-associated metabolites revealed broad, significant compositional changes under VOC exposure, including a general accumulation of metabolites such as long-chain alkanes, terpenoids, wax monoesters and medium-chain fatty acids (i.e., suberic acid), among others and a reduction of some of them (i.e., 1-monoacylglycerols). In particular, the observed enrichment in very-long-chain alkanes is especially relevant, as these compounds constitute key structural components of the intracuticular wax fraction and are known to enhance the transpiration barrier by increasing hydrophobicity and reducing cuticular permeability (Jetter et al., 2016; Riederer & Schreiber, 2001).

Notably, quinic acid, a central shikimate/phenylpropanoid feeder metabolite, increased. The direction of these changes suggests a compensatory response aimed at reinforcing non-stomatal water barriers, since both the composition, namely the chain-length distribution and class balance, and the presence of specific cuticular wax fractions, rather than their total amount alone, determine cuticular permeability (Shepherd and Wynne Griffiths, 2006; Riederer and Schreiber, 2001; Jetter and Riederer, 2016; Kim et al., 2007). In previous experiments, the experimental separation of epi- and intracuticular waxes has shown that the transpiration barrier resides primarily in the intracuticular fraction and depends strongly on the proportion of very-long-chain aliphatics (Jetter and Riederer, 2016; Zeisler-Diehl et al., 2018), which aligns with the observed increase in alkane-type species. Because

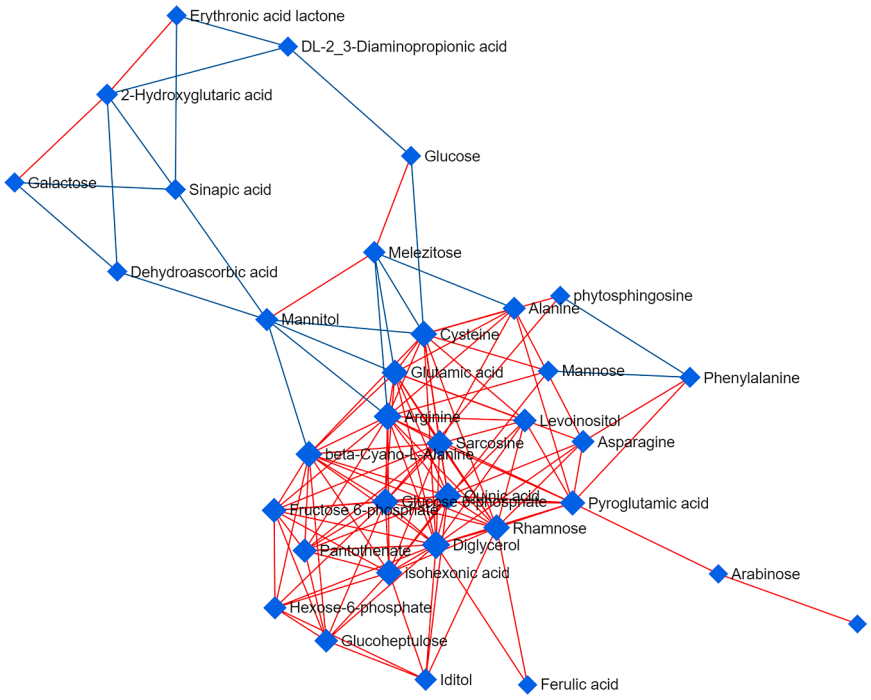

Fig. 6. Correlation network generated by DSPC algorithm based on the metabolites identified in *A. retroflexus* plants exposed to *P. atripicifolia* volatiles. Blue nodes represent metabolites, red lines indicate a positive correlation between metabolites, and blue lines indicate a negative correlation. N=3.

organic volatiles can themselves modify cuticular permeability (Riederer and Schreiber, 2001), the compositional plasticity we detect may reflect a feedback stabilisation of water relations under VOC stress.

Untargeted metabolomics provides a coherent biochemical explanation for the physiological shift. The multivariate structure effectively separated VOC-exposed plants from controls, and univariate contrasts identified dozens of altered metabolites, with a significant signature in phenylpropanoid-linked intermediates. Pathway analysis confirmed a significant enrichment, among others, of "phenylpropanoid biosynthesis" together with amino acid, glutathione/sulfur, and carbohydrate pathways. The phenylpropanoid pathway directs carbon from the shikimate/chorismate hub [fed by quinate and shikimate esters through HCT (Hydroxycinnamoyl-CoA: shikimate hydroxycinnamoyl transferase) enzyme] toward lignin monomers and diverse phenolics that facilitate stress adaptation (Dixon and Paiva, 1995; Vogt, 2010; Hoffmann et al., 2004). The induction of phenylalanine ammonia-lyase activity and the increase in total phenolics in treated plants further suggest the activation of the phenylpropanoid pathways. The increase in lignin content integrates these upstream cues into a structural outcome that is widely associated with enhanced barrier properties and stress resistance (Boerjan et al., 2003; Miedes et al., 2014; Malinovsky et al., 2014; Yadav, S., & Chattopadhyay, 2023). In ecological volatile contexts, phenylpropanoid activation fits with the broader notion that airborne signals and allelochemicals can prime or induce defence networks in exposed plants (Arimura et al., 2009; Ninkovic et al., 2021). The DSPC network analysis further corroborates this interpretation by showing that metabolites central to redox control, nitrogen handling, and phenylpropanoid entry points occupy topological positions expected for coordination hubs under stress. In our network, mannitol exhibits the highest betweenness, indicating a key bridging role among modules consistent with its well-known function as a compatible osmolyte and reactive oxygen species buffer. Cysteine, arginine, glutamate, and pyroglutamate also have a high degree/betweenness, highlighting sulfur assimilation/glutathione metabolism and polyamine routes that typically support oxidative and osmotic stress tolerance. These inferences are congruent with foundational work linking mannitol to osmoprotection and reactive oxygen species scavenging (Stoop et al., 1996; Abebe et al., 2003), glutathione and cysteine metabolism to redox homeostasis (Noctor et al., 2014; Noctor and Foyer, 1998), and arginine-derived polyamines and proline metabolism to stress acclimation (Szabados and Savouré, 2010; Gill and Tuteja, 2010).

Despite its strong depletion, mannitol exhibits the highest betweenness in the network, indicating a key bridging role among metabolic modules. Mannitol is a well-established compatible osmolyte and ROS-buffering metabolite (Alhudhaibi et al., 2024; Abebe et al., 2003), and its central topological position could suggest that it functions as an important hub linking carbohydrate metabolism with stress-related pathways. Its depletion under VOC exposure, combined with its high betweenness, could support the speculation of a substantial reallocation of carbon resources away from osmoprotection and soluble carbohydrate pools toward defence-related and structural metabolism, including phenylpropanoid biosynthesis. Within the phenylpropanoid branch, sinapic acid, a direct precursor of syringyl (S) lignin units, also shows notable centrality in our graph, consistent with the measured lignin increase and with the functional placement of sinapate esters in monolignol biosynthesis (Boerjan et al., 2003; Yadav, S., & Chattopadhyay, 2023). For clarity, degree centrality here quantifies how many direct edges connect a node (metabolite) to others, i.e., its local connectedness, while betweenness centrality measures how frequently a node lies along the shortest paths linking other metabolites, i.e., its potential to control information flow across modules (Freeman, 1977; Newman, 2010; Basu et al., 2017). The use of partial-correlation-based graphs to interpret metabolomics covariance patterns is well established, enabling the distinction between direct and indirect associations (Krumsiek et al., 2011; Basu et al., 2017).

Taken together, these results outline a consistent picture. We observed early inhibition of germination and root elongation, confirming the potential phytotoxic effects during seedling establishment. On the other hand, in developed seedlings, we observed a reprogramming of cuticular wax composition toward very-long-chain aliphatics, the activation of polyphenol oxidase and phenylalanine ammonia-lyase, accompanied by the accumulation of phenolics, and pathway-level enrichment of phenylpropanoid and phenylalanine metabolism. Network analysis further highlighted the central role of osmoprotective

and phenylpropanoid nodes.

These findings support a model in which *P. atriplicifolia* volatiles initially impose chemical stress that hampers the establishment of *A. retroflexus*. In response, the receiving plant reallocates carbon and reducing power to phenylpropanoid–lignin biosynthesis, reinforcing cell walls and limiting further damage.

This model is chemically in agreement with the SPME-HS-GC-MS profile we characterised. For example, oxygenated monoterpenes, such as 1,8-cineole, and hydrocarbon monoterpenes such as o-cymene and δ-3-carene (abundant in our blend), are implicated in germination and root growth inhibition (Verdeguer et al., 2020). Similarly, acetate esters (e.g., geranyl acetate) commonly co-occur in phytotoxic essential oils that inhibit germination and root elongation in receiver species (Martino et al., 2010; Verdeguer et al., 2020; Santonja et al., 2019; Romagni et al., 2000; Kordali et al., 2007). Given that volatile cues can also act as plant-to-plant signals that prime defence pathways, including phenylpropanoid metabolism, it is reasonable that the lignification we detect functions as an adaptive barrier, mechanically strengthening tissues and reducing apoplastic diffusion, rather than as an incidental by-product (Arimura et al., 2009; Dixon and Paiva, 1995; Boerjan et al., 2003; Miedes et al., 2014; Yadav, S., & Chattopadhyay, 2023). Altogether, the data suggest that *P. atriplicifolia* VOC exposure is associated with reduced emergence and early growth of *A. retroflexus*, accompanied by activation of phenylpropanoid metabolism, increased lignin deposition, and cuticular remodelling. These coordinated responses are consistent with a stress-adaptive reprogramming of the receiving species under volatile exposure.

Although the present study highlights a clear metabolic and structural reprogramming of *A. retroflexus* under exposure to *P. atriplicifolia* volatiles, the temporal hierarchy of these responses remains to be fully resolved. Future studies should investigate (i) the temporal dynamics of these responses to distinguish early signaling events from downstream structural adjustments, (ii) the potential uptake and metabolic fate of specific donor-derived volatiles in receiver tissues, and (iii) the possibility of bidirectional volatile interactions under more ecologically complex conditions.

Funding

The European EU-Horizon project “AGROSUS: AGROecological strategies for SUStainable weed management in key European crop” funded the research under Grant Agreement Number 101084084.

Data availability statement

All data supporting the findings of this study are included within the manuscript and its supplementary materials. Additional raw datasets are available from the corresponding author upon reasonable request.

Ai assistance acknowledgement

AI tools were used exclusively for language editing purposes, including correcting grammar and enhancing textual clarity and readability. They were not used to generate text, develop ideas, interpret or analyse data, or perform any other substantive scientific task.

Conflict of Interest Disclosure

The authors declare that they have no financial or non-financial competing interests that could in any way influence the work reported in this paper.

CRediT authorship contribution statement

Alice Zambelli: Writing – review & editing, Validation, Software, Investigation, Formal analysis. **Emanuela Talarico:** Writing – review & editing, Validation, Software, Investigation, Formal analysis. **Cristina Teruzzi:** Writing – review & editing, Software, Investigation, Formal analysis. **Eleonora Greco:** Writing – review & editing, Software, Formal analysis. **David López-González:** Writing – review & editing, Software, Investigation, Formal analysis. **Yedra Vieites-Álvarez:** Writing – review & editing, Software, Investigation, Formal analysis. **Ahmad Arzani:** Writing – review & editing, Visualization, Data curation. **Sara Álvarez-Rodríguez:** Writing – review & editing, Software, Investigation, Formal analysis. **Fabio F. Nocito:** Writing – review & editing, Visualization, Data curation. **Leonardo Bruno:** Writing – review & editing, Visualization, Supervision, Methodology, Data curation, Conceptualization. **Fabrizio Araniti:** Writing – review & editing, Writing – original draft, Supervision, Resources, Project administration, Methodology, Funding acquisition, Data curation, Conceptualization.

Declaration of competing interest

The authors declare that they have no known competing financial interests or personal relationships that could have appeared to influence the work reported in this paper.

Supplementary materials

Supplementary material associated with this article can be found, in the online version, at doi:10.1016/j.stress.2026.101382.

References

Abebe, T., Guenzi, A.C., Martin, B., Cushman, J.C., 2003. Tolerance of mannitol-accumulating transgenic wheat to water stress and salinity. Plant Physiol. 131, 1748–1755. https://doi.org/10.1104/pp.102.003616.

Alhudhaibi, A.M., Ibrahim, M.A., Abd-Elaziz, S.M., Farag, H.R., Elsayed, S.M., Ibrahim, H.A., Srour, H.A., 2024. Enhancing salt stress tolerance in wheat (*Triticum aestivum*) seedlings: insights from trehalose and mannitol. BMC Plant Biol. 24 (1), 472.

Araniti, F., Graña, E., Reigosa, M.J., Sánchez-Moreiras, A.M., Abenavoli, M.R., 2013a. Individual and joint activity of terpenoids, isolated from *Calamintha nepeta* extract, on *Arabidopsis thaliana*. Nat. Prod. Res. 27, 2297–2303. https://doi.org/10.1080/14786419.2013.827193.

Araniti, F., Lupini, A., Mercati, F., Statti, G.A., Abenavoli, M.R., 2013b. *Calamintha nepeta* L.(Savi) as source of phytotoxic compounds: bio-guided fractionation in identifying biological active molecules. Acta Physiol. Plant 35, 1979–1988. https://doi.org/10.1007/s11738-013-1236-7.

Araniti, F., Lupini, A., Sunseri, F., Abenavoli, M.R., 2017. Allelopatic potential of *Dittrichia viscosa* (L.) W. Greuter mediated by VOCs: a physiological and metabolomic approach. PLoS One 12. https://doi.org/10.1371/journal.pone.0170161.

Arimura, G-I., Matsui, K., Takabayashi, J., 2009. Chemical and molecular ecology of herbivore-induced plant volatiles: proximate factors and their ultimate functions. Plant Cell Physiol. 50, 911–923. https://doi.org/10.1093/pcp/pcp030.

Arzani, V., Soleimani, M., Fritsch, T., Jacob, U.M., Calabrese, V., Arzani, A., 2025. Plant polyphenols, terpenes, and terpenoids in oral health. Open Med. 20. https://doi.org/10.1515/med-2025-1183.

Asplund, R.O., 1969. Some quantitative aspects of the phytotoxicity of monoterpenes. Weed Sci. 17, 454–455. https://doi.org/10.1017/S0043174500054539.

Basu, S., Duren, W., Evans, C.R., Burant, C.F., Michailidis, G., Karnovsky, A., 2017. Sparse network modeling and metscape-based visualization methods for the analysis of large-scale metabolomics data. Bioinformatics 33, 1545–1553. https://doi.org/10.1093/bioinformatics/btx012.

Bergman, M.E., Huang, X.-Q., Baudino, S., Caissard, J.-C., Dudareva, N., 2025. Plant volatile organic compounds: emission and perception in a changing world. Curr. Opin. Plant Biol. 85. https://doi.org/10.1016/j.pbi.2025.102706.

Boerjan, W., Ralph, J., Baucher, M., 2003. Lignin biosynthesis. Annu. Rev. Plant Biol. 54, 519–546. https://doi.org/10.1146/annurev.arplant.54.031902.134938.

Brosset, A., Blande, J.D., 2022. Volatile-mediated plant–plant interactions: volatile organic compounds as modulators of receiver plant defence, growth, and reproduction. J. Exp. Bot. 73, 511–528. https://doi.org/10.1093/jxb/erab487.

Chiapusio, G., Sanchez, A., Reigosa, M., Gonzalez, L., Pellissier, F., 1997. Do germination indices adequately reflect allelochemical effects on the germination process? J. Chem. Ecol. 23, 2445–2453. https://doi.org/10.1023/B:JOEC.0000006658.27633.15.

Costea, M., Weaver, S.E., Tardif, F.J., 2004. The biology of Canadian weeds. 130. *Amaranthus retroflexus* L., A. powellii S. Watson and A. hybridus L. Canadian J. Plant. Sci. 84, 631–668. https://doi.org/10.4141/P02-183.

Dabiri, M., Sefidkon, F., 2001. Analysis of the essential oil from aerial parts of *Perovskia atriplicifolia* Benth. At different stages of plant growth. Flav. Fragr. J. 16 (6), 435–438. https://doi.org/10.1002/ffj.988.

de Souza, A.L.C., de Matos, C.H.C., Campos e Silva, R., 2022. Volatile allelochemicals. Essential oils: applications and trends in food science and technology. Springer International Publishing, Cham, pp. 247–261.

D'Cunha, G.B., Satyanarayan, V., Nair, P.M., 1996. Stabilization of phenylalanine ammonia lyase containing *rhodotorula glutinis* cells for the continuous synthesis of L-phenylalanine methyl ester/96. Enzyme Microb. Technol. 19, 421–427. https://doi.org/10.1016/S0141-0229(96)00013-0.

Dixon, R.A., Paiva, N.L., 1995. Stress-induced phenylpropanoid metabolism. Plant Cell 7.

Effah, E., Holopainen, J.K, McCormick, A.C., 2019. Potential roles of volatile organic compounds in plant competition. Perspect Plant Ecol. Evol. Syst. 38, 58–63.

Foster, C.E., Martin, T.M., Pauly, M., 2010. Comprehensive compositional analysis of plant cell walls (lignocellulosic biomass) part I: lignin. JoVE. https://doi.org/10.3791/1745.

Freeman, L.C., 1977. A set of measures of centrality based on betweenness. Sociometry 35–41. https://doi.org/10.2307/3033543.

Gao, Y., Zhuo, R., Luo, H., Ho, C.-T., Chen, Y.L., Zhou, H., Qu, Z., Chen, H., Yi, Y., Wang, Y., Peng, X., Zhu, M., Liu, Z., Xiao, Y., 2025. Characterizing and decoding the effects of co-culture fermentation on dark tea infusion flavor development: elucidating microbial succession and metabolic dynamics mediated by *eurotium cristatum* and water kefir. Food Chem. X 30, 102876. https://doi.org/10.1016/j.fochx.2025.102876.

Gershenzon, J., Dudareva, N., 2007. The function of terpene natural products in the natural world. Nat. Chem. Biol. 3 (7), 408–414. https://doi.org/10.1038/nchembio.2007.5.

Gill, S.S., Tuteja, N., 2010. Polyamines and abiotic stress tolerance in plants. Plant Signal Behav. 5, 26–33. https://doi.org/10.4161/psb.5.1.10291.

Gladikostić, N., Ikonić, B., Teslić, N., Zeković, Z., Božović, D., Putnik, P., Bursać Kovačević, D., Pavlić, B., 2023. Essential oils from Apiaceae, Asteraceae, Cupressaceae and Lamiaceae families grown in Serbia: comparative chemical profiling with in vitro antioxidant activity. Plants 12. https://doi.org/10.3390/plants12040745.

Gostin, I.N., Popescu, I.E., 2025. Russian sage revealed: exploring biology, cultivation, and chemical dimensions of *Salvia yangii*. Agronomy 15, 868. https://doi.org/10.3390/agronomy15040868.

Guo, P., Al-Khatib, K., 2003. Temperature effects on germination and growth of redroot pigweed (*Amaranthus retroflexus*), Palmer amaranth (*A. palmeri*), and common waterhemp (*A. rudis*). Weed Sci. 51, 869–875. https://www.jstor.org/stable/4046740.

Haas, R.A., Crișan, I., Vârban, D., Vârban, R., 2024. Aerobiology of the family Lamiaceae: novel perspectives with special reference to volatiles emission. Plants 13, 1687.

Hodges, D.M., DeLong, J.M., Forney, C.F., Prange, R.K., 1999. Improving the thiobarbituric acid-reactive-substances assay for estimating lipid peroxidation in plant tissues containing anthocyanin and other interfering compounds. Planta 207, 604–611. https://doi.org/10.1007/s004250050524.

Hoffmann, L., Besseau, S., Geoffroy, P., Ritzenthaler, C., Meyer, D., Lapierre, C., Pollet, B., Legrand, M., 2004. Silencing of hydroxycinnamoyl-coenzyme A shikimate/quinate hydroxycinnamoyltransferase affects phenylpropanoid biosynthesis. Plant Cell 16, 1446–1465. https://doi.org/10.1105/tpc.020297.

Islam, A.M., Suttiyut, T., Anwar, M.P., Juraimi, A.S., Kato-Noguchi, H., 2022. Allelopathic properties of Lamiaceae species: prospects and challenges to use in agriculture. Plants 11 (11), 1478. https://doi.org/10.3390/plants11111478.

Jetter, R., Riederer, M., 2016. Localization of the transpiration barrier in the epi-and intracuticular waxes of eight plant species: water transport resistances are associated with fatty acyl rather than alicyclic components. Plant Physiol. 170, 921–934. https://doi.org/10.1104/pp.15.01699.

Karban, R., 2007. Experimental clipping of sagebrush inhibits seed germination of neighbours. Ecol. Lett. 10, 791–797. https://doi.org/10.1111/j.1461-0248.2007.01068.x.

Kim, K.S., Park, S.H., Jenks, M.A., 2007. Changes in leaf cuticular waxes of sesame (*Sesamum indicum* L.) plants exposed to water deficit. J. Plant Physiol. 164, 1134–1143. https://doi.org/10.1016/j.jplph.2006.07.004.

Kordali, S., Cakir, A., Sutay, S., 2007. Inhibitory effects of monoterpenes on seed germination and seedling growth. Z. Naturforsch. C. 62, 207–214. https://doi.org/10.1515/znc-2007-3-409.

Krumsiek, J., Suhre, K., Illig, T., Adamski, J., Theis, F.J., 2011. Gaussian graphical modeling reconstructs pathway reactions from high-throughput metabolomics data. BMC Syst. Biol. 5, 21. https://doi.org/10.1186/1752-0509-5-21.

Landi, M., 2017. Commentary to:"improving the thiobarbituric acid-reactive-substances assay for estimating lipid peroxidation in plant tissues containing anthocyanin and other interfering compounds" by Hodges et al.,. Planta (1999) 207: 604–611 Planta 245. https://doi.org/10.1007/s00425-017-2699-3, 1067-1067.

Landi, M., Araniti, F., Flamini, G., Piccolo, E.L., Trivellini, A., Abenavoli, M.R., Guidi, L., 2020. Help is in the air": volatiles from salt-stressed plants increase the reproductive success of receivers under salinity. Planta 251, 48. https://doi.org/10.1007/s00425-020-03344-y.

Lavergne, F.D., Broeckling, C.D., Cockrell, D.M., Haley, S.D., Peairs, F.B., Jahn, C.E., Heuberger, A.L., 2018. GC-MS metabolomics to evaluate the composition of plant cuticular waxes for four *Triticum aestivum* cultivars. Int. J. Molecul. Sci. 19, 249. https://doi.org/10.3390/ijms19020249.

Lee, B.R., Kim, K.Y., Jung, W.J., Avice, J.C., Ourry, A., Kim, T.H., 2007. Peroxidases and lignification in relation to the intensity of water-deficit stress in white clover (*Trifolium repens* L.). J. Exp. Bot. 58, 1271–1279. https://doi.org/10.1093/jxb/erl280.

Li, T., Holopainen, J.K., Kokko, H., Tervahauta, A.I., Blande, J.D., 2012. Herbivore-induced aspen volatiles temporally regulate two different indirect defences in neighbouring plants. Func. Ecol. 26, 1176–1185. https://doi.org/10.1111/j.1365-2435.2012.01984.x.

Linhart, Y.B., Gauthier, P., Keefover-Ring, K., Thompson, J.D., 2015. Variable phytotoxic effects of *Thymus vulgaris* (Lamiaceae) terpenes on associated species. Int. J. Plant Sci. 176 (1), 20–30. https://doi.org/10.1086/678772.

Lisec, J., Schauer, N., Kopka, J., Willmitzer, L., Fernie, A.R., 2006. Gas chromatography mass spectrometry–based metabolite profiling in plants. Nat. Prot. 1, 387–396. https://doi.org/10.1038/nprot.2006.59.

Maffei, M., Camusso, W., Sacco, S., 2001. Effect of *Mentha× piperita* essential oil and monoterpenes on cucumber root membrane potential. Phytochem 58, 703–707. https://doi.org/10.1016/S0031-9422(01)00313-2.

Malinovsky, F.G., Fangel, J.U., Willats, W.G., 2014. The role of the cell wall in plant immunity. Front. Plant Sci. 5, 178. https://doi.org/10.3389/fpls.2014.00178.

Martino, L.D., Mancini, E., de Almeida, L.F.R., Feo, V.D., 2010. The antigerminative activity of twenty-seven monoterpenes. Molecul 15, 6630–6637. https://doi.org/10.3390/molecules15096630.

Miedes, E., Vanholme, R., Boerjan, W., Molina, A., 2014. The role of the secondary cell wall in plant resistance to pathogens. Front. Plant Sci. 5, 358. https://doi.org/10.3389/fpls.2014.00358.

Misra, B., 2019. Steps for building an open source EI-MS mass spectral library for GC-MS-based metabolomics. Protocols io. https://doi.org/10.17504/protocols.io.8txhwpn.

Misra, B.B., Das, V., Landi, M., Abenavoli, M., Araniti, F., 2020. Short-term effects of the allelochemical umbelliferone on *Triticum durum* L. metabolism through GC–MS based untargeted metabolomics. Plant Sci. 298, 110548. https://doi.org/10.3390/plants9101347.

Mobarak, S.H., Basit, A., Gui, S.H., Hu, C.X., Yu, X.L., Felton, G.W., Liu, T.X., 2025. Volatile organic compounds as mediators in plant-herbivore interactions: mechanisms and evolutionary consequences. Entomol. Gen. https://doi.org/10.1127/entomologia/3516.

Muller, W.H., Muller, C.H., 1964. Volatile growth inhibitors produced by Salvia species. Bull Torrey Bot. Club 327–330. https://doi.org/10.2307/2484047.

Newman, M.E., 2010. Networks: an introduction. Oxford University Press. https://doi.org/10.1093/acprof:oso/9780199206650.001.0001.

Ninkovic, V., Markovic, D., Rensing, M., 2021. Plant volatiles as cues and signals in plant communication. Plant Cell Environ. 44, 1030–1043. https://doi.org/10.1111/pce.13910.

Nishida, N., Tamotsu, S., Nagata, N., Saito, C., Sakai, A., 2005. Allelopathic effects of volatile monoterpenoids produced by *Salvia leucophylla*: inhibition of cell proliferation and DNA synthesis in the root apical meristem of Brassica campestris seedlings. J. Chem. Ecol. 31, 1187–1203. https://doi.org/10.1007/s10886-005-4256-y.

Noctor, G., Foyer, C.H., 1998. Ascorbate and glutathione: keeping active oxygen under control. Annu. Rev. Plant Biol. 49, 249–279. https://doi.org/10.1146/annurev.arplant.49.1.249.

Noctor, G., Mhamdi, A., Foyer, C.H., 2014. The roles of reactive oxygen metabolism in drought: not so cut and dried. Plant Physiol. 164, 1636–1648. https://doi.org/10.1016/j.scienta.2017.10.009.

Pierik, R., Ballaré, C.L., Dicke, M., 2014. Ecology of plant volatiles: taking a plant community perspective. Plant Cell Environ. 37, 1845–1853. https://doi.org/10.1111/pce.12330.

Rattray, R.D, Van Wyk, B.E., 2021. The botanical, chemical and ethnobotanical diversity of southern African Lamiaceae. Molecules 26, 3712. https://doi.org/10.3390/molecules26123712.

Riederer, M., Schreiber, L., 2001. Protecting against water loss: analysis of the barrier properties of plant cuticles. J. Exp. Bot. 52, 2023–2032. https://doi.org/10.1093/jexbot/52.363.2023.

Romagni, J.G., Allen, S.N., Dayan, F.E., 2000. Allelopathic effects of volatile cineoles on two weedy plant species. J. Chem. Ecol. 26, 303–313. https://doi.org/10.1023/A:1005414216848.

Sairam, R., Srivastava, G., Agarwal, S., Meena, R., 2005. Differences in antioxidant activity in response to salinity stress in tolerant and susceptible wheat genotypes. Biol. Plant 49, 85–91. https://doi.org/10.1007/s10535-005-5091-2.

Samani, M.R., Cerulli, A., Serreli, G., Melis, M.P., Deiana, M., Masullo, M., Piacente, S., 2025. *Perovskia atriplicifolia* benth (russian sage), a source of diterpenes exerting antioxidant activity in caco-2 cells. Plants 14, 2795. https://doi.org/10.3390/plants14172795.

Santonja, M., Bousquet-Mélou, A., Greff, S., Ormeño, E., Fernandez, C., 2019. Allelopathic effects of volatile organic compounds released from *Pinus halepensis* needles and roots. Ecol. Evol. 9, 8201–8213. https://doi.org/10.5061/dryad.s0b179p.

Schulz, M., Kussmann, P., Knop, M., Kriegs, B., Gresens, F., Eichert, T., Ulbrich, A., Marx, F., Fabricius, H., Goldbach, H., 2007. Allelopathic monoterpenes interfere with *Arabidopsis thaliana* cuticular waxes and enhance transpiration. Plant Signal Behav. 2, 231–239.

Shepherd, T., Wynne Griffiths, D., 2006. The effects of stress on plant cuticular waxes. New Phytol. 171, 469–499. https://doi.org/10.4161/psb.2.4.4469.

Silva, E., Overbeck, G., Soares, G., 2014. Phytotoxicity of volatiles from fresh and dry leaves of two Asteraceae shrubs: evaluation of seasonal effects. S. Afr. J. Bot. 93, 14–18. https://doi.org/10.1016/j.sajb.2014.03.006.

Singh, H.P., Batish, D.R., Kaur, S., Arora, K., Kohli, R.K., 2006. α-pinene inhibits growth and induces oxidative stress in roots. Ann. Bot. 98, 1261–1269. https://doi.org/10.1093/aob/mcl213.

Singleton, V.L., Rossi, J.A., 1965. Colorimetry of total phenolics with phosphomolybdic-phosphotungstic acid reagents. Am. J. Enol. Vitic. 16, 144–158. https://doi.org/10.5344/ajev.1965.16.3.144.

Siriphanich, J., Kader, A.A., 1985. Effects of CO_2 on cinnamic acid-4-hydroxylase in relation to phenolic metabolism in lettuce tissue. J. Am. Soc. Hortic. Sci. 110, 333–335. https://doi.org/10.21273/JASHS.110.3.333.

Souza-Alonso, P., González, L., López-Nogueira, A., Cavaleiro, C., Pedrol, N., 2018. Volatile organic compounds of *Acacia longifolia* and their effects on germination and early growth of species from invaded habitats. Chem. Ecol. 34, 126–145. https://doi.org/10.1080/02757540.2017.1404584.

Stoop, J.M., Williamson, J.D., Pharr, D.M., 1996. Mannitol metabolism in plants: a method for coping with stress. Trends Plant Sci. 1, 139–144. https://doi.org/10.1016/S1360-1385(96)80048-3.

Sumner, L.W., Amberg, A., Barrett, D., Beale, M.H., Beger, R., Daykin, C.A., Fan, T.W.M., Fiehn, O., Goodacre, R., Griffin, J.L., 2007. Proposed minimum reporting standards for chemical analysis: chemical analysis working group (CAWG) metabolomics standards initiative (MSI). Metabolomics 3, 211–221. https://doi.org/10.1007/s11306-007-0082-2.

Szabados, L., Savouré, A., 2010. Proline: a multifunctional amino acid. Trends Plant Sci. 15, 89–97. https://doi.org/10.1016/j.tplants.2009.11.009.

Verdeguer, M., Sánchez-Moreiras, A.M., Araniti, F., 2020. Phytotoxic effects and mechanism of action of essential oils and terpenoids. Plants 9, 1571. https://doi.org/10.3390/plants9111571.

Vogt, T., 2010. Phenylpropanoid biosynthesis. Molecul. Plant 3, 2–20. https://doi.org/10.1093/mp/ssp106.

Wang, C., Liu, Z., Wang, Z., Pang, W., Zhang, L., Wen, Z., Zhao, Y., Sun, J., Wang, Z.Y., Yang, C., 2022. Effects of autotoxicity and allelopathy on seed germination and seedling growth in *Medicago truncatula*. Front., Plant Sci. 13, 908426. https://doi.org/10.3389/fpls.2022.908426.

Werrie, P.Y., Durenne, B., Delaplace, P., Fauconnier, M.L., 2020. Phytotoxicity of essential oils: opportunities and constraints for the development of biopesticides. A review. Foods 9, 1291. https://doi.org/10.3390/foods9091291.

Wielkopolan, B., Jakubowska, M., Dobosz, R., Bocianowski, J., Bruzzoniti, M.C., Mayhew, C.A., Narloch, I., Dawidowicz, K., Piesik, D., 2025. The effects of biotic and abiotic stress on the emission of volatile organic compounds by sugar beet plants. J. Plant Prot. Res. 65, 2.

Xiao, Y., Chen, H., Chen, Y., Ho, C.-T., Wang, Y., Cai, T., Li, S., Ma, J., Guo, T., Zhang, L., Liu, Z., 2024. Effect of inoculation with different *Eurotium cristatum* strains on the microbial communities and volatile organic compounds of Fu brick tea. Food Res. Int. 197 (Pt 1), 115219. https://doi.org/10.1016/j.foodres.2024.115219.

Xiao, Y., Huang, Y., Chen, Y., Zhu, M., He, C., Li, Z., Wang, Y., Liu, Z., 2022. Characteristic fingerprints and change of volatile organic compounds of dark teas during solid-state fermentation with *eurotium cristatum* by using HS-GC-IMS, HS-SPME-GC-MS, E-nose and sensory evaluation. LWT 169, 113925. https://doi.org/10.1016/j.lwt.2022.113925.

Xie, Y., Tian, L., Han, X., Yang, Y., 2021. Research advances in allelopathy of volatile organic compounds (VOCs) of plants. Horticulture 7, 278. https://doi.org/10.3390/horticulturae7090278.

Yadav, S., Chattopadhyay, D., 2023. Lignin: the building block of defense responses to stress in plants. J. Plant Growth Regul. 42 (10), 6652–6666. https://doi.org/10.1007/s00344-023-10926-z.

Yang, Y., Sun, F., Hu, C., Gao, J., Wang, W., Chen, Q., Ye, J., 2025. Emissions of biogenic volatile organic compounds from plants: impacts of air pollutants and environmental variables. Curr. Pollut. Rep. 11, 10. https://doi.org/10.1007/s40726-024-00339-1.

Yoshimura, H., Sawai, Y., Tamotsu, S., Sakai, A., 2011. 1, 8-cineole inhibits both proliferation and elongation of BY-2 cultured tobacco cells. J. Chem. Ecol. 37, 320–328. https://doi.org/10.1007/s10886-011-9919-2.

Zeisler-Diehl, V., Müller, Y., Schreiber, L., 2018. Epicuticular wax on leaf cuticles does not establish the transpiration barrier, which is essentially formed by intracuticular wax. J. Plant Physiol. 227, 66–74. https://doi.org/10.1016/j.jplph.2018.03.018.